

## ASSESSMENT OF CROPLAND TRANSITION TO SOLAR FARMS AND OTHER LAND USE/COVER USING RS, GIS AND ANN-CA

J. A. Principe<sup>1\*</sup>, M. E. Sotto<sup>2</sup>, I. B. Benitez<sup>2</sup>

<sup>1</sup> Dept. of Geodetic Engineering, College of Engineering, University of the Philippines Diliman, Philippines - japrincipe@up.edu.ph

<sup>2</sup> National Engineering Center, University of the Philippines Diliman, Philippines - (mesotto, ibbenitez)@up.edu.ph

**KEY WORDS:** cropland, solar farm, ANN-CA, MOLUSCE, MCD12Q1, nighttime lights, LandScan

### ABSTRACT:

The balance between food security and energy security is a national issue of extreme importance. A more stable supply of electricity could be achieved as solar farms expand but at the expense of losing some of the prime agricultural lands which endangers availability of sufficient agricultural produce. This study aims to use ANN-Cellular Automata (CA) via the Geographic Information System (GIS) platform and remote sensing (RS) data to assess the impact of cropland transition to solar farms and other land use/land cover (LULC). Several remotely sensed data were processed including MODIS land cover data (MCD12Q1), VIIRS nighttime lights (VNL v2.1), Advanced Himawari Imager Shortwave Radiation (AHI-SWR) product, and population density (LandScan) as inputs to the Cellular Automata-Artificial Neural Network (CA-ANN) model to simulate LULC changes in Tarlac Province, Philippines via the Modules for Land Use Change Evaluation (MOLUSCE) plugin in QGIS. For years 2019, 2023 and 2027 with 2015 as the base year, results showed an increasing trend for savannas and grassland with  $\Delta$ LULC values of +11.4% to +15.1% and +0.2% to 3.5%, respectively. Meanwhile, a decreasing trend is observed for built-up/water, forest, and cropland with  $\Delta$ LULC values of -3.0% to -6.3%, -8.5% to -21.1%, and -3.9% to -4.2%, respectively. Results also showed a conversion of a 100-ha area of croplands to solar farm from year 2019 to 2023 which translates to an estimated monetary loss from agricultural produce due to solar farm conversion amounting to Php 7,584,720.00 (~USD 138,000) which is equivalent to the total average annual income of about 67 families in Tarlac. Lastly, the simulated 2027 LULC map showed pixels with unrealistic conversions from solar farm (year 2023) to cropland (year 2027). To improve the model, it is recommended to add more spatial data to effectively capture factors that may contribute to the expansion of solar farms in the future. Moreover, high resolution LULC maps (vector maps if available) can be used instead of a coarse resolution satellite-derived raster data. Nonetheless, this study has demonstrated the use of RS, GIS and machine learning techniques to model cropland conversion to solar farms and other LULC classes. Results from this study can provide scientific data to policy makers, solar industry players and other relevant stakeholders in doing technoeconomic assessment of solar farm development and expansion considering its effect on energy security and food security towards national sustainable development.

### 1. INTRODUCTION

Food security and energy security are two of the most pressing global issues of today. The United Nations Sustainable Development Goals (SDGs) seek to address these concerns by providing goals targeting to end all forms of poverty everywhere, achieve food security, and guarantee everyone's access to affordable, reliable, sustainable, and modern energy (United Nations, 2015). To meet the growing demand for energy, countries around the world have been utilizing renewable sources of energy. However, conversion of agricultural lands to solar power plants poses serious concerns with regards to food security. It is for this reason that the Philippine Department of Agrarian Reform (DAR) proposed a two-year moratorium on land conversions (Gomez, E. J., 2019). Therefore, there is a need to assess how much agricultural areas have been converted to different uses (e.g., energy use) and how it can negatively affect food security while trying to meet legitimate needs of the nation (e.g., energy supply).

The integration of remotely-sensed data and geographic information system (GIS) has become a powerful tool in land use/land cover (LULC) change analysis for different applications including, but not limited to, its impact on vegetation cover, urban expansion, deforestation, food security and energy security (Hussain, S. et al., 2020; Guo, L. et al., 2021; Hassan, Z. et al., 2016; de Luna, A. D. et al., 2021). Meanwhile, machine learning algorithms such as artificial

neural networks (ANN) have been extensively used for LULC change studies with satellite data as important inputs (Muhammad, R. et al., 2022; Kamaraj, M. and Rangarajan, S., 2022; Megahed, Y. et al., 2015).

The Advanced Himawari Imager (AHI-8) is a multipurpose moderate resolution geostationary imager which operators across the 16 channels from the visible to the infrared regions with wavelengths of 470 nm to 13.30  $\mu$ m and bandwidth of 20 nm to 0.37  $\mu$ m (JAXA-EORC, 2015; Bessho et al., 2016). Shortwave Radiation / Photosynthetically Available Radiation (SWR/PAR) product of AHI-8 is derived from a model proposed by Frouin and Murakami (2007) which uses plane-parallel radiative transfer theory (Frouin and Murakami, 2007; Takenaka et al., 2011). Studies of Yu et al (2018) and Zhang et al (2022) showed that AHI-8 product exhibits the highest level of accuracy when validated with ground data and compared to other satellite data such as MERRA-2, CERES-SYN and ERA-Interim.

Machine learning (ML) techniques such as random forest (RF), neural networks (NN), support vector machine (SVM), maximum likelihood classifier (MLC), decision trees, and K-Nearest Neighbors (KNN) (Gislason et al., 2006; Svoboda et al., 2022; Kulkarni and Lowe, 2016; Storie and Henry, 2018; Alshari et al., 2023; Taati, A. et al. 2015; Norovsuren, B. et al., 2019; Friedl and Brodley, 1997; Srimani and Prasad, 2012; Upadhyay et al., 2016) have been used for land use/land cover

mapping due to its high accuracy and efficiency. Moreover, NN and Artificial Neural Networks (ANN) are often used interchangeably on machine learning applications. ANN demonstrated to be particularly effective in classifying different types of land use/land cover and has been used in various studies for mapping land use/cover, including the use of remotely sensed data (Alshari et al., 2023; Mishra et al., 2018; Kadavi and Lee, 2018; Rojas et al., 2020; Dede et al., 2022). A study by Kadavi and Lee (2018) found that ANN outperformed SVM. The same observation was supported by Ge et al (2020), where ANN had the highest accuracies compared to other three machine learning algorithms (RF, KNN, SVM).

To date, there has been no significant study done yet to quantify and model the expansion of solar farms using machine learning, RS and GIS techniques. As such, this study aims to use ANN-Cellular Automata (CA) via the GIS platform and remote sensing data to assess the transition of croplands to solar farms and other LULC. Results of this study can provide scientific information to relevant stakeholders in both the agriculture and energy sectors with regards to formulating policies and plans to achieve food security and energy security.

## 2. STUDY AREA

The study area covers the city of Tarlac, and municipalities of Capas, Concepcion, Gerona, La Paz, Pura and Victoria (Fig. 1). Two large solar power plants are currently operating in the area namely, the PetroSolar/Tarlac City and Concepcion Solar Power Plants. Tarlac province is home to more than 107,000 hectares of agricultural farms as of 2002 (NSO, 2012).

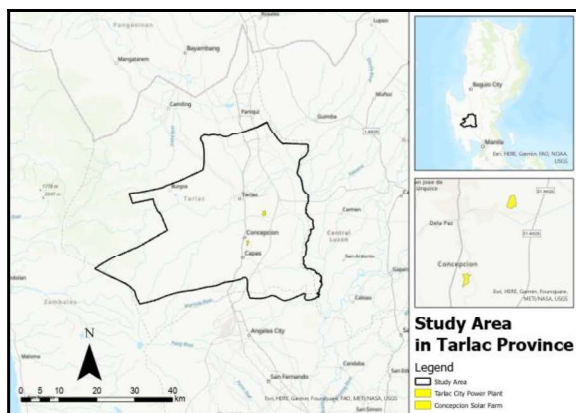


Figure 1. Study area in Tarlac Province, Philippines.

## 3. METHODOLOGY

### 3.1 Data

Three satellite products are used in this study summarized in Table 1.

Data	Description	Resolution	Year
MCD12Q1	Land cover types	500m	2015, 2019
VNL (v2.1)	Nighttime lights	500m	2019
AHI-SWR	Shortwave radiation	5 km	2019
LandScan	Population density	1 km	2019

Table 1. Satellite data used in this study.

MCD12Q1 Land Cover Type Product is a global land cover dataset at 500-m spatial resolution generated by performing a

supervised classification on Moderate Resolution Imaging Spectroradiometer (MODIS) reflectance data. The said product was downloaded from the Land Processes Distributed Active Archive Center (LP DAAC) of NASA's Earth Observing System Data and Information System (EOSDIS) (L.P. DAAC, 2019). Five LULC classes are defined in this study: built-up/water (no solar PV installation areas), forest, savanna, cropland, grassland, and solar power plants (SPP).

Meanwhile, the version 2.1 of the annual global Visible and Infrared Imaging Suite (VIIRS) nighttime lights (VNL) was an upgrade of Version 2, corrected for a bug in calculating for the annual average radiance filtering technique (Elvidge et al., 2021). VNL data was downloaded from the Earth Observation Group of Payne Institute for Public Policy (<https://eogdata.mines.edu/products/vnl>).

Lastly, the shortwave radiation (SWR) is a product from Advanced Himawari Imager (AHI) 8/9 (AHI-SWR) and downloaded via the JAXA Himawari Monitor (<http://eorc.jaxa.jp/ptree/index.html>). The AHI-SWR has a spatial resolution of 5 km and temporal resolution ranging from 10-minutes to 1-month for the full disk extent. Each raster contains multiple bands which includes data on the total atmosphere optical thickness, total atmosphere angstrom exponent, photosynthetically active radiation, shortwave radiation, ultraviolet-A radiation, ultraviolet-B radiation (JAXA-EORC, 2015; Bessho et al., 2016). Level 3 monthly data of the AHI-8 SWR/PAR product is derived from the hourly data at each pixel. Raster Calculator from the Raster analysis tools in QGIS was then used in this study to process the annual SWR data of the Philippines from the AHI-8 L3 SWR monthly NetCDF rasters. The resolution, spatial extent and output coordinate reference system were copied and calculated from the existing raster data.

### 3.2 Methods

The general methodology used in this study is shown in Fig. 2. Satellite data were downloaded and resampled to 500-m spatial resolution and clipped to the study area's boundary. Pixels in the 2019 land cover dataset were manually edited to reflect the actual location of solar farms via the Serval plugin in QGIS and later assigned a separate pixel value (i.e., "5"). The MOLUSCE plugin in QGIS was then launched. The Modules for Land Use Change Evaluation (MOLUSCE) is an open-source plugin for QGIS 2.0 and above, developed by Asia Air Survey Co., Ltd. designed to analyse, model, and simulate LULC changes (Gismondi, M. et al., 2014). The 2015 and 2019 LC data were assigned as "Initial" and "Final" LULC dataset, respectively, while data on nighttime lights, population density and shortwave radiation were assigned as "Spatial variables". Next is the evaluation of correlation among the input variables, computation for area changes, transition potential modelling using ANN (multi-layer perceptron) method, and CA simulation.

Cellular automata (CA) is a mathematical model consisting of a network of cells, each with a state that changes over time according to a set of rules (Wolfram, 1983). CA is used in land use/land cover studies to simulate changes in territory cover over time due to variables like population increase, urban development, and climate change (Guzman et al., 2020; Pratomoatmojo, 2018; Pinto et al., 2021). Moreover, studies combined cellular automata-artificial neural networks, termed as the CA-ANN method, with the ANN predicting the possible outcomes of transitions in the CA model (Norizah et al., 2023;

Yang et al., 2016; Sajan et al., 2022). This method is known to be useful for forecasting changes in land use/land cover and can aid in long-term management and planning efforts.

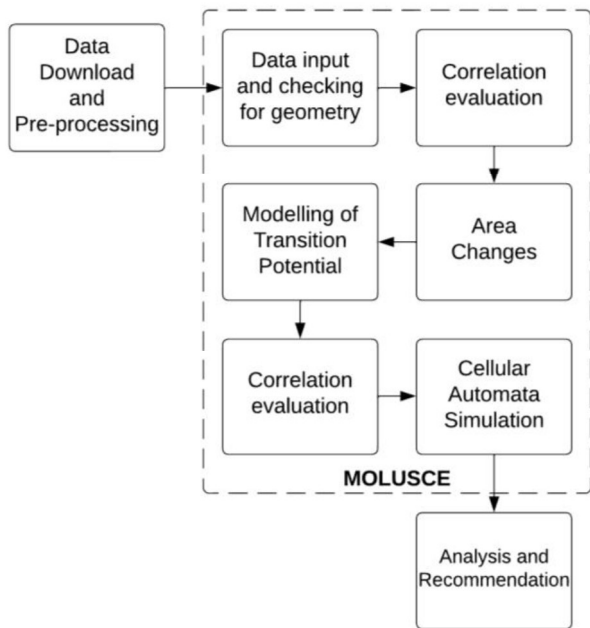


Figure 2. General methodology of this study.

The calibrated CA-ANN model was run to simulate the LULC distribution for the year 2023 using the input data for years 2015 and 2019. Since there is no available MCD12Q1 data yet for year 2023, the simulated LULC map was compared with latest high resolution satellite image from Google Earth with emphasis on the possible expansion of solar farms. The model was rerun to simulate a LULC map for the study area for year 2027 this time using input data for years 2019 and 2023.

Percent change in land use/cover for a particular year compared to the base year (i.e., 2015) was computed per LULC class using Eq. (1):

$$\Delta LULC_{i,j,k} = \frac{\sum Pixel_{k,j} - \sum Pixel_{k,i}}{\sum Pixel_{k,i}} \times 100\% \quad (1)$$

where  $\Delta LULC_{i,j,k}$  is the percentage change in a LULC class  $k$  for a preceding year  $j$  as compared to the base year  $i$ ,  $Pixel_{k,i}$  and  $Pixel_{k,j}$  are the pixel values assigned to class  $k$  for years  $i$  and  $j$ , respectively.

Moreover, Eq. (2) is used to compute for the estimated monetary loss from agricultural produce due to solar farm conversion:

$$P_{loss} = A_{loss} \times Y \times P_{farmgate} \times 1000 \quad (2)$$

where  $P_{loss}$  is the monetary equivalent of agricultural produce lost due to solar farm conversion,  $Y$  is the palay yield per hectare (tons/ha), and  $P_{farmgate}$  is the average farmgate price of palay (dry) (Php/kg), and 1000 is the unit conversion factor for tons to kg.

Lastly, further analyses were done from which recommendations would be based.

## 4. RESULTS AND DISCUSSIONS

### 4.1 Correlation of data inputs and area changes

Among the three spatial variables, the nighttime lights (VNL) and population density (PD) had the highest Pearson's correlation value of 0.54, followed by shortwave radiation (SWR) and PD (0.21); while SWR and VNL had the lowest correlation (0.16).

Fig. 3 shows the cropland conversions to grassland, savanna and SPP corresponding to 0.9%, 5.5%, and 0.4% LC changes, respectively.

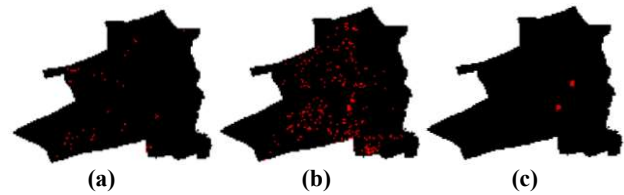
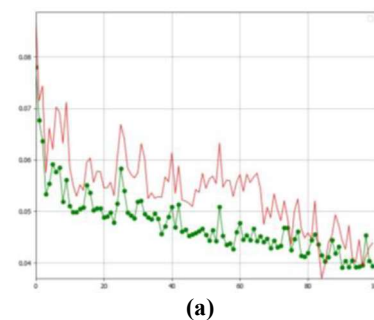


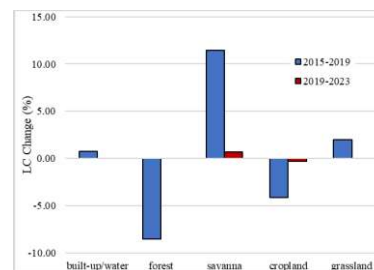
Figure 3. Cropland conversions (2015-2019) to (a) grassland, (b) savanna, and (c) solar power plants.

### 4.2 Transition potential mapping and simulation

The transition potential modelling was done via the ANN multi-layer perceptron which was optimized with the following parameter values: neighbourhood = 1 px; learning rate = 0.010; maximum iterations = 100; hidden layers = 5; momentum = 0.060; current validation kappa = 0.82. The neural network learning curve is shown in Fig. 4a. Meanwhile, Fig. 4b shows the LULC transition for 2015-2019 (actual) and 2019-2023 (simulated). This simulation showed a further decrease in cropland areas to about 0.28% from 2019 or -4.39% from 2015.



(a)



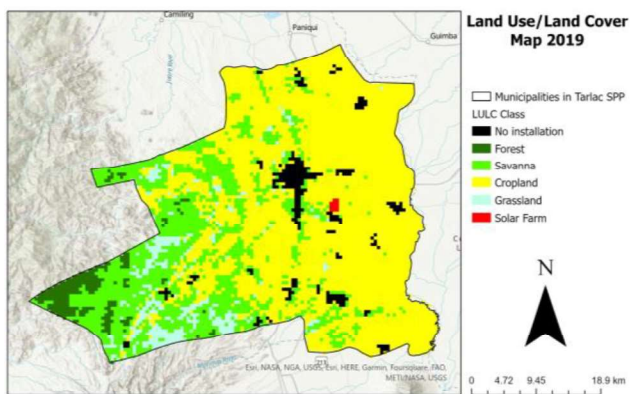
(b)

Figure 4. Result of transition potential modelling in MOLUSCE: (a) Neural network learning curve, (b) LULC transitions.

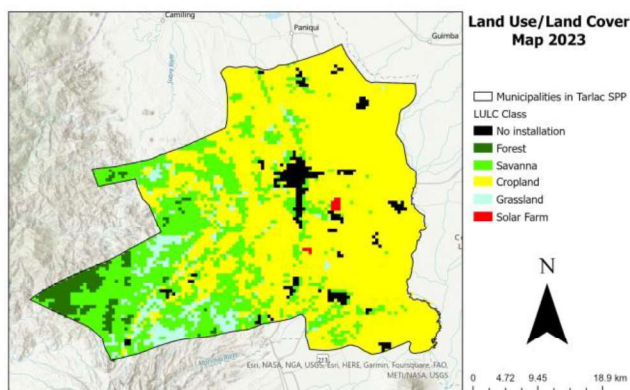
The LULC map for 2019 is shown in Fig. 5 together with the resulting maps from the model runs for the years 2023 and 2027. The said maps show a seemingly unchanged distribution

of LULC classes through the time periods considered. However, upon closer inspection, new four pixels solar farms can be seen as having been added in year 2023 in a span of four years (i.e., 2019-2023). These new solar farms pixels can be translated to about 100 hectares of land which are previously croplands. Based on the latest satellite image from Google Earth Pro, these pixels are indeed located in the new solar farms called Concepcion Solar and Sta. Rosa Solar being operated by Solar Philippines Tarlac Corporation and Terasu Energy Inc which have been in commercial operation since February 2020 and January 2022, respectively (DOE, 2021; DOE, 2022).

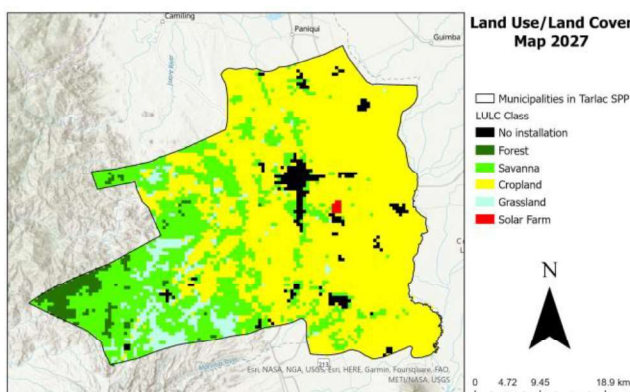
According to the Philippine Statistics Authority, the palay yield in Tarlac is 4.29 metric tons/ha as of the third quarter of 2022 while the average farmgate price of palay (dry) is at Php 17.68/kg as of December 2022 (PSA, 2022; PSA 2023). Assuming that the estimated 100-ha area that were previously planted with rice, Tarlac being one of the country's major rice-producing provinces (Mamiit et al, 2021), the estimated monetary loss from agricultural produce due to solar farm conversion is  $P_{loss} = \text{Php } 7,584,720.00$  which is equivalent to the total average annual income of about 67 families in Tarlac province based on statistical data (NSO, 2008).



(a)



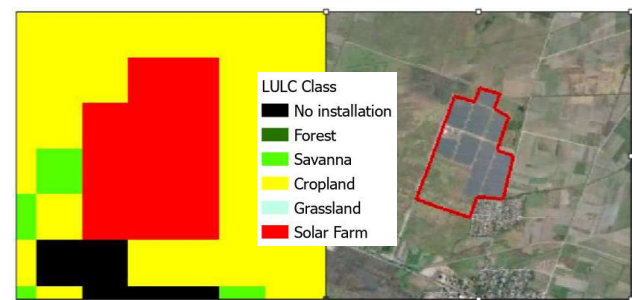
(b)



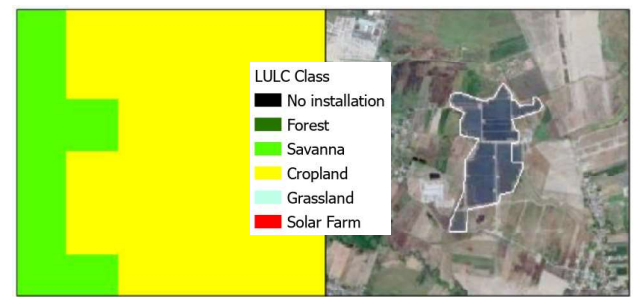
(c)

**Figure 5.** Land use/land cover map for the years (a) 2019, (b) 2023 and (c) 2027. The last two maps were simulated using the Cellular Automata in MOLUSCE plugin.

In the 2027 simulation of LULC, it is apparent that some of the solar farm pixels remain as is, but some were replaced by other LULC class including cropland (Fig. 6). Although it is possible, this conversion type (i.e., solar farm to cropland) is highly unlikely as evidenced by the latest satellite imagery of the same area. With this observation, a refinement of the model is deemed needed. It is recommended to add more spatial data as inputs to the CA-ANN model including road network, digital elevation model, energy transmission/distribution line network, among others. If historical and most recent LULC maps in shapefile format are available from the concerned government agency (e.g., such as the Philippine National Mapping and Resource Information Authority), these can be used as initial and final LULC maps as opposed to the coarse spatial resolution of MCD12Q1 raster data.



(a)



(b)

**Figure 6.** Predicted of LULC map for year 2027: (a) realistic prediction since solar farm remains as is; (b) unrealistic prediction since solar farm is converted back to cropland.

Fig. 7 shows the percentage of LULC changes for years 2019, 2023 and 2027 with 2015 as the base year. In general, there is an observed increasing trend for savannas and grassland with  $\Delta\text{LULC}$  values of +11.4% to +15.1% and +0.2% to 3.5%, respectively. Meanwhile, a decreasing trend is observed for built-up/water, forest, and cropland with  $\Delta\text{LULC}$  values of -3.0% to -6.3%, -8.5% to -21.1%, and -3.9% to -4.2%, respectively. As there are no savannas in the Philippines, the two classes—savannas and woody savannas—as defined in the

IGBP system can be attributed to the percent of canopy/vegetation cover with the latter having higher percentage than the former. As such, in dealing with these classes, their percentage of vegetation canopy cover can be used to indicate possible conversion to solar farms, with the decrease in canopy cover suggesting a high possibility of conversion from vegetation to solar farm.

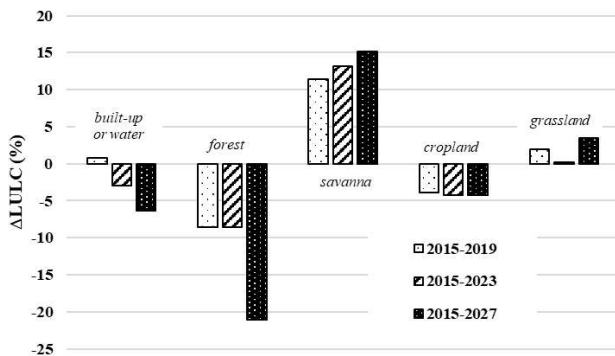


Figure 7. Percentage of LULC changes from 2015.

## 5. CONCLUSION AND RECOMMENDATION

This study utilized various remotely sensed products, GIS and machine learning techniques to assess the impact of cropland conversion to solar farms. Specifically, satellite-derived data on land cover types (MCD12Q1), nighttime lights (VNL v2.1), shortwave radiation (AHI-SWR), and population density (LandScan) were inputs to the MOLUSCE plugin in QGIS to simulate via the CA-ANN algorithm the LULC changes in Tarlac Province, Philippines. In terms of LULC change rate, it is observed that there is an increasing trend for savannas and grassland with  $\Delta$ LULC values of +11.4% to +15.1% and +0.2% to 3.5%, respectively. Meanwhile, a decreasing trend is observed for built-up/water, forest, and cropland with  $\Delta$ LULC values of -3.0% to -6.3%, -8.5% to -21.1%, and -3.9% to -4.2%, respectively. Results also showed a conversion of a 100-ha area of croplands to solar farm from year 2019 to 2023 which translates to an estimated monetary loss from agricultural produce due to solar farm conversion amounting to Php 7,584,720.00 (~USD 138,000) which is equivalent to the total average annual income of about 67 families in Tarlac. Lastly, the simulated 2027 LULC Map showed pixels with unrealistic conversions from solar farm (year 2023) to cropland (year 2027). It is therefore recommended to add more spatial data to effectively factors that may contribute to the expansion of solar farms in the future. Moreover, high resolution LULC maps (vector maps if available) can be used instead of a course resolution satellite-derived raster data. Nonetheless, this study has demonstrated the use of RS, GIS and machine learning techniques to model cropland conversion to solar farms. Results from this study can provide scientific data to policy makers, solar industry players and other relevant stakeholders of both agriculture and solar energy in doing technoeconomic assessment of solar farm development and expansion considering its effect on energy security and food security towards national sustainable development.

## ACKNOWLEDGMENTS

This study was done through the FF Cruz Prof. Chair in Geodetic Engineering. The authors wish to thank the NASA's

Earth Observing System Data and Information System (EOSDIS) for the MODIS Land Cover (MCD12Q1) product, the Earth Observation Group of Payne Institute for Public Policy for the VNL data, the Japan Aerospace Exploration Agency (JAXA) for the SWR data, and the University of the Philippines for the license to use ArcGIS Pro. Lastly, the DOST-Science Education Institute (DOST-SEI) Engineering Research and Development for Technology (ERDT) Program for the research dissemination grant.

## REFERENCES

- Alshari, E. A., Abdulkareem, M. B., and Gawali, B. W., 2023: Classification of land use/land cover using artificial intelligence (ANN-RF), *Front. Artif. Intell.*, vol. 5. <https://www.frontiersin.org/articles/10.3389/frai.2022.964279> (Feb. 27, 2023).
- Bessho, K., Date, K., Hayashi, M., Ikeda, A., Imai, T., Inoue, H., Kumagai, Y., Miyakawa, T., Murata, H., Ohno, T., Okuyama, A., Oyama, R., Sasaki, Y., Shimazu, Y., Shimoji, K., Sumida, Y., Suzuki, M., Taniguchi, H., Tsuchiyama, H., Uesawa, D., Yokota, H., and Yoshida, R., 2016: An Introduction to Himawari-8/9— Japan's New-Generation Geostationary Meteorological Satellites. *Journal of the Meteorological Society of Japan*, 94, pp. 151-183.
- Dede, M., Asdak, C. and Setiawan, I., 2022: Spatial dynamics model of land use and land cover changes: A comparison of CA, ANN, and ANN-CA, *Regist. J. Ilm. Teknol. Sist. Inf.*, vol. 8, no. 1, Art. no. 1. doi: 10.26594/register.v8i1.2339.
- de Luna, A. D., Pascual, C. E. B., Principe, J. A., and Ang, M. R. C. O. (2021). "COST-BENEFIT ANALYSIS OF CONVERTING AGRICULTURAL LAND INTO SOLAR FARM USING RS & GIS: CASE OF TARLAC PROVINCE," *Int. Arch. Photogramm. Remote Sens. Spatial Inf. Sci.*, XLVI-4/W6-2021, pp. 133–140; <https://doi.org/10.5194/isprs-archives-XLVI-4-W6-2021-133-2021>.
- DOE, 2021. LIST OF EXISTING POWER PLANTS (GRID-CONNECTED) AS OF DECEMBER 2020. Department of Energy. <https://www.doe.gov.ph/list-existing-power-plants> (25 February 2023).
- DOE, 2022. LIST OF EXISTING POWER PLANTS (GRID-CONNECTED) AS OF NOVEMBER 2022. Department of Energy. <https://www.doe.gov.ph/list-existing-power-plants> (25 February 2023).
- Elvidge, C.D, Zhizhin, M., Ghosh, T., Hsu, FC, and Taneja, J., 2021: Annual time series of global VIIRS nighttime lights derived from monthly averages: 2012 to 2019. *Remote Sensing* 13(5), pp. 1-14.
- Friedl, M. A., and Brodley, C. E., 1997: Decision tree classification of land cover from remotely sensed data, *Remote Sens. Environ.*, vol. 61, no. 3, pp. 399–409. doi: 10.1016/S0034-4257(97)00049-7.
- Frouin, R. and Murakami, H., 2007: Photosynthetically Available Radiation Algorithm: Estimating photosynthetically available radiation at the ocean surface from ADEOS-II global imager data. *J. Oceanography*, 63, pp. 493-503.
- Ge, G., Shi, Z., Zhu, Y., Yang, X., and Hao, Y., 2020: Land

- use/cover classification in an arid desert-oasis mosaic landscape of China using remote sensed imagery: Performance assessment of four machine learning algorithms, *Glob. Ecol. Conserv.*, vol. 22, p. e00971. doi: 10.1016/j.gecco.2020.e00971.
- Gislason, P. O., Benediktsson, J. A. and Sveinsson, J. R., 2006: Random Forests for land cover classification. *Pattern Recognit. Lett.*, vol. 27, no. 4, pp. 294–300. doi: 10.1016/j.patrec.2005.08.011.
- Gismondi, M., Kamusoko, C., Furuya, T. et al., 2014: MOLUSCE an open source land use change analyst for QGIS. Asia Air Survey Co., Ltd, Tokyo.
- Gomez, E.J., 2019. Land conversion memo out next month–DAR. [https://www.manilatimes.net/2019/02/21/business/business-top/land-conversion-memo-out-next-month-dar/514634/\(23-Feb-2021\)](https://www.manilatimes.net/2019/02/21/business/business-top/land-conversion-memo-out-next-month-dar/514634/(23-Feb-2021)).
- Guo, L., Xi, X., Yang, W., Liang, L., 2021: Monitoring Land Use/Cover Change Using Remotely Sensed Data in Guangzhou of China. *Sustainability* 13, 2944. <https://doi.org/10.3390/su13052944>
- Guzman, L. A., Escobar, F., Peña, J. and Cardona, R., 2020: A cellular automata-based land-use model as an integrated spatial decision support system for urban planning in developing cities: The case of the Bogotá region, *Land Use Policy*, vol. 92, p. 104445. doi: 10.1016/j.landusepol.2019.104445.
- Hassan, Z., Shabbir, R., Ahmad, S.S. et al., 2016: Dynamics of land use and land cover change (LULCC) using geospatial techniques: a case study of Islamabad Pakistan. *SpringerPlus* 5(812). <https://doi.org/10.1186/s40064-016-2414-z>
- Hussain, S., Mubeen, M., Akram, W. et al., 2020: Study of land cover/land use changes using RS and GIS: a case study of Multan district, Pakistan. *Environ Monit Assess* 192(2). <https://doi.org/10.1007/s10661-019-7959-1>.
- JAXA-EORC, 2015. JAXA Himawari Monitor P-Tree System User Guide. Japan Aerospace Exploration Agency, Earth Observation Research Center. <https://www.eorc.jaxa.jp/ptree/userguide.html> (27 February 2023).
- Kadavi, P. R. and Lee, C.W., 2018: Land cover classification analysis of volcanic island in Aleutian Arc using an artificial neural network (ANN) and a support vector machine (SVM) from Landsat imagery, *Geosci. J.*, vol. 22, no. 4, pp. 653–665. doi: 10.1007/s12303-018-0023-2.
- Kamaraj, M. and Rangarajan, S., 2022: Predicting the future land use and land cover changes for Bhavani basin, Tamil Nadu, India, using QGIS MOLUSCE plugin. *Environ Sci Pollut Res.* <https://doi.org/10.1007/s11356-021-17904-6>.
- Kulkarni, A. D., and Lowe, B., 2016: Random Forest Algorithm for Land Cover Classification,” *Int. J. Recent Innov. Trends Comput. Commun.*, vol. 4, no. 3.
- L.P. DAAC, 2019. MCD12Q1 MODIS/Terra+Aqua Land Cover Type Yearly L3 Global 500m SIN Grid V006 [Data set]. <https://doi.org/10.5067/MODIS/MCD12Q1.006>.
- Mamiit, R. J., Yanagida, J., and Miura, T., 2021: Productivity Hot Spots and Cold Spots: Setting Geographic Priorities for Achieving Food Production Targets. *Front. Sustain. Food Syst.*, 5, pp.1-15. doi: <https://doi.org/10.3389/fsufs.2021.727484>.
- Megahed, Y., Cabral, P., Silva, J., and Caetano, M., 2015: Land Cover Mapping Analysis and Urban Growth Modelling Using Remote Sensing Techniques in Greater Cairo Region—Egypt. *ISPRS Int. J. Geo-Inf.*, 4, 1750-1769. doi:10.3390/ijgi4031750.
- Mishra, V. N., Rai, P. K., Prasad, R., Punia, M., and Nistor, M. M., 2018: Prediction of spatio-temporal land use/land cover dynamics in rapidly developing Varanasi district of Uttar Pradesh, India, using geospatial approach: a comparison of hybrid models, *Appl. Geomat.*, vol. 10, no. 3, pp. 257–276. doi: 10.1007/s12518-018-0223-5.
- Muhammad, R., Zhang, W., Abbas, Z., Guo, F., Gwiazdzinski, L., 2022: Spatiotemporal Change Analysis and Prediction of Future Land Use and Land Cover Changes Using QGIS MOLUSCE Plugin and Remote Sensing Big Data: A Case Study of Linyi, China. *Land* 11 (419). <https://doi.org/10.3390/land11030419>.
- Norizah, K., Jamhuri, J., Balqis, M., Mohd Hasmadi, I. and Nor Akmar, A. A., 2023: Land Use and Land Cover Change Prediction Using ANN-CA Model,” in *Tropical Forest Ecosystem Services in Improving Livelihoods For Local Communities*, Z. Samdin, N. Kamaruddin, and S. M. Razali, Eds. Singapore: Springer Nature, pp. 107–125. doi: 10.1007/978-981-19-3342-4\_7.
- Norovsuren, B., Tseveen, B., Batomunkuev, V., Renchin, T., Natsagdorj, E., Yangiv, A., and Mart, Z., 2019: Land cover classification using maximum likelihood method (2000 and 2019) at Khandgait valley in Mongolia,” *IOP Conf. Ser. Earth Environ. Sci.*, vol. 381, no. 1, p. 012054. doi: 10.1088/1755-1315/381/1/012054.
- NSO, 2008. TARLAC QUICKSTAT. Databank and Information Services Division, NSO, Quezon City. <https://www.psa.gov.ph/sites/default/files/attachments/ird/quickstat/Decemembr.pdf> (01 Mar. 2023).
- NSO, 2012. TARLAC QUICKSTAT. Databank and Information Services Division, NSO, Quezon City. [https://psa.gov.ph/sites/default/files/attachments/ird/quickstat/tarlac\\_may12.pdf](https://psa.gov.ph/sites/default/files/attachments/ird/quickstat/tarlac_may12.pdf) (30 Sept. 2022).
- Pinto, N., Antunes, A. P., and Roca, J., 2021: A Cellular Automata Model for Integrated Simulation of Land Use and Transport Interactions, *ISPRS Int. J. Geo-Inf.*, vol. 10, no. 3, Art. no. 3. doi: 10.3390/ijgi10030149.
- Pratomoatmojo, N. A., 2018: LanduseSim Algorithm: Land use change modelling by means of Cellular Automata and Geographic Information System, *IOP Conf. Ser. Earth Environ. Sci.*, vol. 202, no. 1, p. 012020. doi: 10.1088/1755-1315/202/1/012020.
- PSA, 2022. Palay and Corn Situation in Tarlac. <http://rsso03.psa.gov.ph/tags/corn-and-palay-situation-tarlac> (01 Mar. 2023).
- PSA, 2023. Updates on Farmgate Prices of Palay (Dry) December 2022. <https://psa.gov.ph/farmgate-prices-palay/node/176400> (01 Mar. 2023).
- Rojas, F., Rubio, C., Rizzo, M., Bernabeu, M., Akil, N., and Martín, F., 2020: Land Use and Land Cover in Irrigated

- Drylands: a Long-Term Analysis of Changes in the Mendoza and Tunuyán River Basins, Argentina (1986–2018), *Appl. Spat. Anal. Policy*, vol. 13, no. 4, pp. 875–899. doi: 10.1007/s12061-020-09335-6.
- Sajan, B., Mishra, V. N., Kanga, S., Meraj, G., Singh, S. K. and Kumar, P., 2022: Cellular Automata-Based Artificial Neural Network Model for Assessing Past, Present, and Future Land Use/Land Cover Dynamics, *Agronomy*, vol. 12, no. 11, Art. no. 11. doi: 10.3390/agronomy12112772.
- Srimani, D. P. K., and Prasad, S. N., 2012: DECISION TREE CLASSIFICATION MODEL FOR LAND USE AND LAND COVER MAPPING- A CASE STUDY, *Int. J. Curr. Res.*, vol. 4.
- Storie, C. D. and Henry, C. J., 2018: "Deep Learning Neural Networks for Land Use Land Cover Mapping," in *IGARSS 2018 - 2018 IEEE International Geoscience and Remote Sensing Symposium*, pp. 3445–3448. doi: 10.1109/IGARSS.2018.8518619.
- Svoboda, J., Štych, P., Laštovička, J., Paluba, D., and Kobliuk, N., 2022: "Random Forest Classification of Land Use, Land-Use Change and Forestry (LULUCF) Using Sentinel-2 Data—A Case Study of Czechia," *Remote Sens.*, vol. 14, no. 5, Art. no. 5. doi: 10.3390/rs14051189.
- Taati, A., Sarmadian, F., Mousavi, A., Pour, C. T. H., and Shahir, A. H. E., 2015: Land Use Classification using Support Vector Machine and Maximum Likelihood Algorithms by Landsat 5 TM Images, *Walailak J Sci & Tech*.
- Takenaka, H., Nakajima, T. Y., Higurashi, A., Higuchi, A., Takamura, T., Pinker, R. T., and Nakajima, T., 2011: Estimation of solar radiation using a neural network based on radiative transfer. *J. Geophys. Res.*, 116, D08215. <https://doi.org/10.1029/2009JD013337>.
- United Nations, 2015: Transforming our World: The 2030 Agenda for Sustainable Development. United Nations, NY.
- Upadhyay, A., Shetty, A., Kumar Singh, S., and Siddiqui, Z., 2016: Land use and land cover classification of LISS-III satellite image using KNN and decision tree. In *2016 3rd International Conference on Computing for Sustainable Global Development (INDIACom)*, Mar. 2016, pp. 1277–1280.
- Wolfram, S., 1983: Statistical mechanics of cellular automata," *Rev. Mod. Phys.*, vol. 55, no. 3, pp. 601–644. doi: 10.1103/RevModPhys.55.601.
- Yang, X., Chen, R., and Zheng, X. Q., 2016: Simulating land use change by integrating ANN-CA model and landscape pattern indices, *Geomat. Nat. Hazards Risk*, vol. 7, no. 3, pp. 918–932. doi: 10.1080/19475705.2014.1001797.
- Yu, Y., J. Shi, T. Wang, H. Letu, P. Yuan, W. Zhou, and L. Hu., 2018: Evaluation of the Himawari-8 Shortwave Downward Radiation (SWDR) Product and its Comparison With the CERES-SYN, MERRA-2, and ERA-Interim Datasets. *IEEE Journal of Selected Topics in Applied Earth Observations and Remote Sensing*, 12 (2), pp. 1–14.
- Zhang, Y. & Chen, L. & Liu, J., 2022: ESTIMATION OF DAILY GLOBAL SOLAR IRRADIANCE FROM HIMAWARI-8 PRODUCTS OVER CHINA. *ISPRS Annals of*